



Discussion of: “Mode II fracture mechanics properties of wood measured by the asymmetric four-point bending test using a single-edge-notched specimen of Hiroshi Yoshihara Eng. Frac. Mech. 75 (2008) 4727–4739”

T.A.C.M. van der Put

Technical University Delft, Faculty of Civil Engineering and Geosciences, Timber Structures and Wood Technology, The Netherlands

ARTICLE INFO

Article history:

Received 8 March 2012

Accepted 9 April 2012

Keywords:

Mode II

Wood

Asymmetric four-point bending test

Single edge-notched beam test

ABSTRACT

A discussion is given of the article mentioned in the title. The conclusions of this article, based on classical fracture mechanics, are shown to be questionable in the light of new theory and the there preferred mode II asymmetric four point bending test is shown to be problematic in giving the right values of fracture toughness and release rate. The in the article given data provide information on equivalent mode II softening behaviour and confirms that the strength of the intact fracture plane then is determining, the same as applies for mode I.

© 2012 Elsevier Ltd. All rights reserved.

1. Introduction

In the here discussed article [1], the “asymmetric four point bending” (AFPB) test is regarded to be the best test for fracture mechanics mode II because it does not show the drawbacks of the mostly applied end-notched flexure (ENF) test. However this conclusion, based on classical fracture mechanics is questionable in the light of new theory. It will be shown that these drawbacks do not exist at proper treatment and that the AFPB test is really problematic in giving the right values of fracture toughness and release rate. However, the data of [1] provide information on equivalent mode II softening behaviour and confirms that the strength of the intact fracture plane then is determining, the same as applies for mode I. To show this, the results of the applied singularity approach has to be discussed in the light of the fracture mechanics theory of [2] leading to a new conclusions.

2. Discussion of the applied singularity approach

The in [1] applied compliance factor:

$$c_{II} = \frac{1}{\sqrt{2}} \sqrt{\sqrt{\frac{E_x}{E_y}} + \frac{1}{2} \left(\frac{E_x}{G_{xy}} - 2\nu_{xy} \right)} \quad (1)$$

in the energy release rate expression:

$$K_{IIc} = \sqrt{\frac{E_x G_{IIc}}{c_{II}}} \quad (2)$$

E-mail address: vanderp@xs4all.nl

is based on the solution of the Airy stress function of [3] by chosen elementary row solutions in polar coordinates in the form of: $f(\theta) \times r^{-0.5}$. The thereof following solution is not unique, but one of the multiple possible solutions of the Airy stress function. A solution of the Airy stress function is in principle not unique, because multiple allowable equilibrium systems, differing an internal equilibrium system from each other and not violating the failure criterion, are possible as (lower bound) solutions. In [2] e.g. a similar solution of the Airy stress function is given, based on the same elementary solutions in the form of: $f(\theta) \times r^{-0.5}$ but now in the real measured material compliances. There thus is no reason to apply Eq. (1). For wood both mentioned solutions may act as lower bound solutions for the most simple loading cases, thus only for uniaxial strengths (at $r = r_0$, the radius of the crack tip). The highest general lower bound solution has to be found because this will be the closest to the real solution. This highest lower bound solution of the Airy stress function, in elliptic coordinates, is given in [2] and is equal to the real solution because it is identical to the Wu-equation of the strength for combined loading, Eq. (11). This last is not the case for all known solutions in polar coordinates which also conflict with the equilibrium conditions of the wood matrix, as is shown in [2]. Thus there only remains one possible solution. According to this (elliptic) continuum mechanics solution of [2], which applies for a crack in a large space, the factor:

$$c_{II} = 1/(4n_6^2) \quad (3)$$

with $n_6 = (2 + \nu_{21} + \nu_{12})(G_{xy}/E_x)$ in Eq. (2), as estimate for the compliance for oblique off axis crack extension. For mode I is $c_I = 1$.

The application in [1] of the wrong factor c_{II} and other schematization errors lead to a wrong value of $f(a/W)$ in:

$$K_{IIc} = \tau_0 \sqrt{\pi a} \cdot f\left(\frac{a}{W}\right) \quad (4)$$

because $f(a/W)$ is not only applied as geometry factor, accounting for the form of the specimen, but is applied as a correction factor:

$$f\left(\frac{a}{W}\right) \equiv \sqrt{\frac{E_x G_{IIc}}{\pi a}} \cdot \frac{1}{\tau_0} \quad (5)$$

This factor hides errors in G_{II} and a . As geometry factor it could be expected that $f(a/W) \approx 1$ for small crack lengths. However this value $f(a/W) \approx 1$ is found at $a/W \approx 0.7$ in [1] and $f(a/W)$ thus is too low due to a too low value of G_{IIc} (although this is compensated by a too low value of a by the input of the nominal value of the crack length a).

Regarding the fracture energy G_{IIc} or G_{Ic} , the following should be realized. When a cantilever is loaded by a load P , at the moment of crack propagation, the beam deforms and the load goes down by an displacement of say δ . The external energy, applied to the beam, then is $P\delta$. The increase of elastic energy is $P\delta/2$. Thus the energy for fracture is: $P\delta - P\delta/2 = P\delta/2$, which is equal to the elastic energy increase. When the external load is prevented to move, the whole elastic energy change is applied as fracture energy. This equality principle is the basis of the (elastic) compliance method and the finite element virtual crack closure method, determining the elastic energy for crack closure as measure of the fracture energy. For full plastic crack extension however, there is no change of elastic energy and all external energy is applied for crack extension. In the case of the cantilever above, the fracture energy then is $P\delta$, twice the elastic estimate. In principle, failure by collinear crack extension due to pure shear loading and pure coaxial shear deformation is plastic in that direction and the fracture energy is twice the assumed and so calculated pure elastic strain energy change by collinear crack extension. Similar to plastic deformation is work dissipation by a high density of small cracks, extending and merging, and thus preventing a rise of the mean stress, similar to plastic flow, as applies e.g. in the fracture process zone or in the whole fracture plane when this is high loaded in the ultimate state. The right “elastic” value of G_{IIc} , based on elastic energy change during crack extension, follows from oblique crack extension, which is coupled to G_{Ic} . Both follow from tensile failure of the crack wall near the crack tip. According to the derivation of the Wu-criterion of [2] therefore is:

$$G_{IIc} = 4G_{Ic} \quad (6)$$

for oblique crack extension (see e.g. Fig. 1) by the ultimate uniaxial plane tangential tensile stress (cohesion strength) at the crack-tip wall. For a flat elliptic crack in a stress field, failure, thus crack extension, occurs there at the crack wall where the tensile stress is maximal and ultimate, σ_t , leading to the expression [2]:

$$1 = \frac{\sigma_y}{\xi_0 \sigma_t / 2} + \frac{\tau_{xy}^2}{\xi_0^2 \sigma_t^2} \quad (7)$$

for stresses in the isotropic wood matrix. For flat cracks is near the crack tip the elliptic coordinate: $\xi_0 = \sqrt{2r_0/c}$, giving in orthotropic stresses:

$$1 = \frac{\sigma_y}{\xi_0 \sigma_t / 2} + \frac{\tau_{ort}^2}{\xi_0^2 \sigma_t^2 n_6^2} = \frac{\sigma_y \sqrt{\pi c}}{\sigma_t \sqrt{2\pi r_0} / 2} + \frac{(\tau_{xy} \sqrt{\pi c})^2}{(\sigma_t n_6 \sqrt{2\pi r_0})^2} = \frac{K_I}{K_{Ic}} + \frac{(K_{II})^2}{(K_{IIc})^2} \quad (8)$$

For $\tau_{xy} = 0$, crack extension is at the crack tip and the (mode I) extension is collinear. For $\sigma_y = 0$, crack extension is just behind the tip and this (mode I) extension is oblique, off axis, perpendicular to the elliptic crack wall but is regarded to be a mode II extension. The same applies for combined stresses, called mixed mode extension.

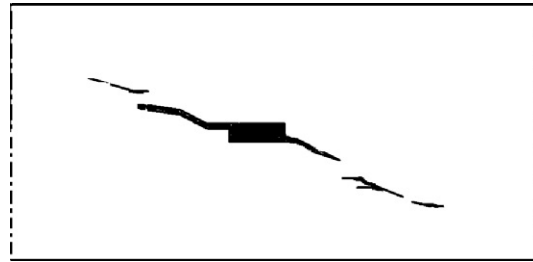


Fig. 1. Shear failure by the asymmetric four point bending test with small center-slit. Sketch after the photo of [4].

Clear wood fracture is always by the same small cracks with the same diameter $2r_0$ and the same initial crack length c and Eq. (8) can be read as the common failure criterion of [6]:

$$1 = \frac{\sigma_y}{f_{t,90}} + \frac{\tau_{xy}^2}{f_v^2} \quad (9)$$

If K_{Ic} and K_{IIc} are material properties, then fracture should be always by the same small cracks, with diameter $2r_0$, at the equivalent cohesion strength σ_r . The small cracks extend towards the macro crack-tip, causing in that way macro-crack propagation.

Thus the stress analysis shows that there always is tensile (mode I) failure for any combined normal stress – shear loading as derived in [2]. Although Eq. (6) is derived for cracks in an infinite medium, it also appears to apply for cracks in specimens with limited dimensions. This is due to the Wu-failure criterion, which applies as well for small cracks (clear wood) as for timber with defects and for macro-cracks in a specimen. This confirms that macro crack propagation is due to small cracks multiplication and merging. The real empirical confirmation of Eq. (6) follows from fracture mechanics research of Gustafsson, showing $G_{IIc} = 3.5G_{Ic}$ (correlation $R^2 = 0.64$), which is smaller than 4, probably due to the regarded too high G_{Ic} – value following from the area under the softening curve. Thus, by not regarding oblique crack extension or “plastic” collinear crack extension at pure shear loading in [1], but treating this by elastic fracture mechanics by calculating the elastic energy change by the finite element virtual crack closure method, possibly a two times too low ratio, thus: $G_{IIc} = 2G_{Ic}$ is found. Other values can be measured depending on the type of test, size and thickness etc. and on the level of (the always present) mixed mode loading part and whether or not the real critical stress state at the top of the loading curve is regarded or the end state of softening (as in AFPB). Mentioned by Yoshihara are values between 1.7 and 2.6.

Because the finite element virtual crack closure technique cannot be applied for critical oblique crack extension, G_{IIc} should follow from Eq. (6) by measuring the G_{Ic} – value. This application will at least gives a reasonable lower bound solution of the strength.

Determining for the strength are flat cracks and fracture mechanics thus is about plane stress and strain problems and uniaxial tensile failure represented by the Wu-equation applying for any combined shear- normal stress loading. Solutions as:

$$\sigma_{ij} = K_{I1}f_1(\theta, c_{ij}) \cdot r^{-0.5} + K_{II}f_2(\theta, c_{ij}) \cdot r^{-0.5} + K_{III}f_3(\theta, c_{ij}) \cdot r^{-0.5} \quad (10)$$

thus do not apply for linear elastic fracture mechanics, not only because this is against the Wu failure criterion, but also because different modes do not apply for oblique, off axis, crack extension. The fully elastic solution, Eq. (11), represents at least an allowable equilibrium system, satisfying compatibility and boundary conditions and nowhere else than in one point reaching the strength criterion, thus is a limit analysis lower bound solution, differing, in principle, a safe internal equilibrium system with the real occurring solution. However, is as lower bound solution equal to the real occurring solution which is identical to Eq. (11).

$$\frac{K_I}{K_{Ic}} + \frac{K_{II}^2}{K_{IIc}^2} = 1 \quad (11)$$

The by the theory predicted property $G_{IIc} = 4G_{Ic}$ thus can be applied for lower bound solutions and is also verified by measurements [2]. Eq. (11) for combined stresses, can be expressed in fracture energies and the determining total critical fracture energy:

$$G_f = G_I + G_{II} \quad (12)$$

according to [2], Chapter 5 as:

$$\frac{K_I}{K_{Ic}} + \frac{K_{II}^2}{K_{IIc}^2} = \frac{\sqrt{G_I}}{\sqrt{G_{Ic}}} + \frac{G_{II}}{G_{IIc}} = \frac{\sqrt{\gamma G_f}}{\sqrt{G_{Ic}}} + \frac{(1 - \gamma)G_f}{4G_{Ic}} = 1 \quad (13)$$

The last three terms represent a quadratic equation in $\sqrt{G_f/G_{Ic}}$ which gives as solution:

$$G_f = 4G_{Ic} / (1 + \sqrt{\gamma})^2 = G_{IIc} / (1 + \sqrt{\gamma})^2 \tag{14}$$

In the last equations is: $G_f = G_I + G_{II} = \gamma G_f + (1 - \gamma)G_f$ and:

$$\frac{\gamma G_f}{(1 - \gamma)G_f} = \frac{K_I^2}{K_{II}^2} \quad \text{or} : \quad \gamma = \frac{1}{1 + (K_{II}^2/K_I^2)} = \frac{1}{1 + (\tau_{xy}^2/\sigma_x^2)} \tag{15}$$

For pure shear, $\gamma = 0$ and it is sufficient to measure only G_{Ic} because $G_{IIc} = 4G_{Ic}$.

3. Discussion of the apparent decrease of the fracture toughness at softening

The strength behaviour of long cracks in [1] appears to be similar to softening behaviour after passing the top of the curve, similar to Fig. 2. For mode I when the specimen is unloaded and reloaded to measure K_{IIc} for further crack propagation in the softened state. For a not decreasing K_{IIc} – value, softening should follow the Griffith locus given by Fig. 3.

The analysis, following [1] then is as follows:

Eq. (4) of [1] is for the top of the loading curve

$$K_{II,0} = \tau_n \sqrt{\pi a_c} \tag{16}$$

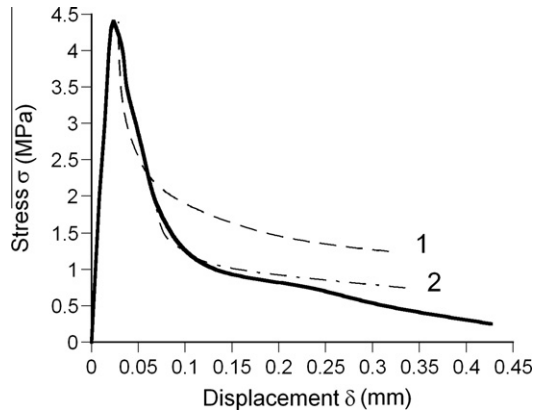


Fig. 2. Stress – displacement of specimen see [2].

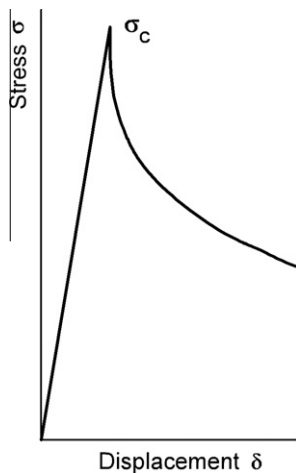


Fig. 3. Softening curve according to Eq. (3.12) of [2].

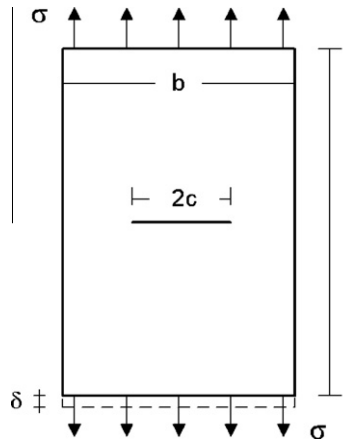


Fig. 4. Specimen $b \times l$ and thickness t , containing a flat crack of $2c$.

because $f(a/W) = 1$ for lower values $a/W < 0.7$. The nominal Griffith shear stress is:

$$\tau_n = 3P/BW \quad (17)$$

As follows from [2], Eq. (3.13), softening occurs at a critical density of cracks, thus when: $a_c = \sqrt{bl/6\pi}$ for mode I, in the dimensions of Fig. 4 below. For the case of [1], $b = W$ and $l = c_1W$, proportional to W , as a St. Venant distance. A similar relation applies for “mode” II, following from the Griffith locus derivation for compression and shear. Thus

$$a_c = \sqrt{Wc_1W/c_2} = c_3W \quad (18)$$

For higher values of a is, as applied in [1]:

$$K_{IIc} = \tau_n \sqrt{\pi a} \cdot f(a/W) \quad (19)$$

It is shown in [2] that after the first stage of softening, K_{II} is not constant any more, but the strength of the decreasing intact area of the fracture plane is determining for the possible loading. Thus not the nominal stress but the ultimate real stress f_t in the fracture plane is determining. Thus Eq. (16) becomes:

$$f_t = K_{II,0}/(\sqrt{\pi a_c} \cdot (1 - a_c/W)) = K_{II,0}/(\sqrt{\pi c_3 W} \cdot (1 - c_3)) \quad (20)$$

and Eq. (19):

$$f_t = K_{II}/(\sqrt{\pi a} \cdot (1 - a/W) \cdot f(a/W)) \quad (21)$$

and from Eqs. (20) and (21) follows:

$$\frac{K_{II}}{\sqrt{\pi a} \cdot (1 - a/W) \cdot f(a/W)} = \frac{K_{II,0}}{\sqrt{\pi c_3 W} \cdot (1 - c_3)} \quad \text{or:} \quad \frac{K_{II}}{\sqrt{a/W} \cdot (1 - a/W) \cdot f(a/W)} = \frac{K_{II,0}}{\sqrt{c_3} \cdot (1 - c_3)} = c_4 \quad (\text{constant}) \quad (22)$$

According to Fig. 12 of [1], there is no difference (by volume effect) between the data for $W = 40$ mm and $W = 20$ mm, thus mean values of both can be regarded.

$$\text{For } a/W = 0.7, \quad K_{II} = 0.79 \text{ MPa}\sqrt{\text{m}} \quad \text{thus: } c_4 = 3.15 \quad (23)$$

$$\text{For } a/W = 0.8, \quad K_{II} = 0.71 \text{ MPa}\sqrt{\text{m}} \quad \text{thus: } c_4 = 3.3 \quad (24)$$

$$\text{For } a/W = 0.9, \quad K_{II} = 0.52 \text{ MPa}\sqrt{\text{m}} \quad \text{thus: } c_4 = 3.28 \quad (25)$$

$f(a/W) = 1.0$ for $a/W = 0.7$ and is 1.2 for $a/W = 0.8$ and is 1.67 for $a/W = 0.9$.

Thus the mean value of c_4 is:

$$c_4 = 3.24 \quad (26)$$

Numerically this calculation is:

$$0.79 / (\sqrt{0.7} \cdot 0.3 \cdot 1) = 3.15 \quad \text{and:} \quad 0.71 / (\sqrt{0.8} \cdot 0.2 \cdot 1.2) = 3.31 \quad \text{and:} \quad 0.52 / (\sqrt{0.9} \cdot 0.1 \cdot 1.67) = 3.28.$$

It thus is confirmed by the data of [1] that, (due to small crack propagation in the fracture plane), the strength of the intact part of the fracture plane is determining and not K_{II} . This result was found before for K_I in [2] based on the softening data of [5].

K_{II} is determining at the top of the loading curve and according to the (ENF) test this is: $1.57 \text{ MPa}\sqrt{\text{m}}$. The theory of [2] thus explains the lower values of K_{II} for long initial crack lengths. The value of $K_{II} = 0.52 \text{ MPa}\sqrt{\text{m}}$ indicates the last small crack joining stage of [2], because K_{II} is reduced by a factor $0.52/1.57 = 0.33$ with respect to the Griffith value at the top of the equivalent loading curve. Also the value of 0.79 for $a/W = 0.7$ is in that softening range of reduced K_{II} , showing an apparent K_{II} – reduction factor of: $0.79/1.57 = 0.5$.

As mentioned the values of 0.57 and 0.79 are expected to be too low, based on the elastic energy change at fracture. This is compensated by the 3ENF-value which also is about the same factor too low, based on a 5% rule, which should not be applied for K_{II} – tests, because this value is too far away from the top of the curve. The value from literature is about $1.9\text{--}2 \text{ MPa}\sqrt{\text{m}}$, thus a factor $2/1.57 = 1.3$ higher.

Based on the possible factor 2 higher fracture energy of [1], the value of K_{II} follows from a $\sqrt{2}$ higher value of c_4 . An optimal value further is $c_3 = 0.33$ and it is possible to choose this as a high lower bound solution. Then Eq. (22) becomes:

$$K_{II0} = c_4 \cdot \sqrt{c_3} \cdot (1 - c_3) = \sqrt{2} \cdot 3.24 \cdot \sqrt{0.33} \cdot 0.667 = 1.76 \text{ MPa}\sqrt{\text{m}}$$

for Spruce. This shows that then the value of $1.57 \text{ MPa}\sqrt{\text{m}}$, according to the 3ENF – 5% rule, is a too low, lower bound.

4. Discussion of the end-notched flexure test

In [1], the so called three-point bend end-notched flexure (3ENF) test (i.e. the single-edge notched beam test, SENB) was done as control on the value of K_{IIc} obtained by the AFPB-test and it was found that the 3ENF-values are more than a factor 2–3 higher. This has to be explained. For an analysis, the 3ENF- loading case is regarded as a result of two different loading cases.

In Fig. 5, the “mode II” test is represented by case $a + a''$. If the sign of the lower reaction force V of this case is reversed and $P = 0$, the loading of the mode I, double cantilever beam (DCB) test is obtained, identical to loading case c with $N = 0$. In Fig. 5, case $a + a''$ is split in case a and in case a'' , as loading of the upper and the lower cantilever. Case a is identical to case a' which is similar to end-notched beams discussed in [2] Chapter 6. This case behaves like the mode I fracture test as can be seen by loading case c . The loading near the crack tip, given by case a , can be seen as the result of superposition of the stresses of cases b and c , where the loading of case b is such, that the un-cracked state of the beam, case b' , occurs. The loading of case c is such that the sum of cases b and c gives loading case a . Case c is the real crack problem and the critical value of strain energy release rate G_c can be found by calculating the differences of elastic strain energies between case a' and b' , the cracked and un-cracked system [2]. Case c shows the loading of the mode I – DCB-test by V and M , combined with shear loading by N and the energy release rate thus will be somewhat smaller (by this combination with N) than the value of the pure DCB-test.

For the loading case a'' , the same stresses occur as in case a , however with opposite directions of M and V with respect to those of case c , according to case c'' , causing crack closure. To prevent that crack closure c'' , and friction, dominates above crack opening c , the crack slit has to be filled with a Teflon sheet. By superposition of cases c and c'' , case $c + c''$ of shear loading of pure mode II occurs, as crack problem due to the total loading. The normal load couple of $2N$ is just the amount to close the horizontal shift of both beam ends with respect to each other at that loading stage. This explains the applicability of the virtual crack closure technique. The fracture energy also can be found by subtraction of elastic energies of the cracked and intact states $a + a''$ and b' (see [2], Chapter 6). The equations of these energies based on the calculated deflections according to the elementary equilibrium equations of the beams are the same for determination of G_{II} as for G_I according to the DCB-test. Only the ultimate loads are different. This will be explained in the following. The elementary equilibrium equations for slender beams can be seen as first terms of a row expansion of the real bending and shear stresses which determine the

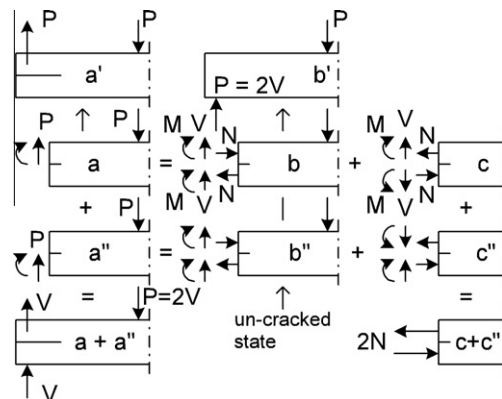


Fig. 5. Fracture loading of the “three-point bend end-notched flexure test (3ENF).

deformation of the beam and thus the work of the external load. The higher order terms need not to be regarded because they form internal equilibrium systems, not contributing in total to the beam deformation. Of course the elastic shear deformation is primary and not negligible in shear failure tests (see [2], Chapter 6) and should be accounted. However, the in [1] mentioned defection by small cracks extension, causing a plastic like dissipation at the crack tip, should not be accounted. This is, just as crack bridging, part of the fracture process within the elastic-“plastic” boundary around the crack and thus is not part of the linear elastic fracture mechanics for crack extension from this boundary. By crack extension of the initial horizontal slit, the original beam is split in two equal smaller beams above each other. Because of the high shear stress, there is sufficient plastic shear deformation of these two beams to make mutual load redistribution possible. Because the compression perpendicular to the grain due to the central load is higher in the upper beam and because the Wu-equation also applies for combined shear with normal stress in grain direction as shown and explained in [6], K_{II} will be higher than K_{IIC} in the upper beam near the crack tip by the influence of compression perpendicular and of bending compression of the intact part of the beam, while this is the reverse for the lower beam under influence of bending tension of the intact part of the beam. This means that system c of Fig. 5 dominates above system c' , and crack extension occurs by tensile mode I at a lower resultant value than K_{Ic} because of the combined failure with shear stress due to N . Failure by the opening mode tensile stress thus also occurs in this apparent pure shear fracture case $c + c'$ of Fig. 5.

5. Conclusions regarding differences between the 3ENF- and AFPB-tests

The Wu-equation is as real solution, the minimum energy solution. Any other forced failure mode, is not according to the Wu-equation and thus needs more energy and is an upper bound solution, violating the failure criterion. In that case the determination of the elastic energy change gives a too low value of the fracture energy. Besides macro-crack extension micro-crack extension may become determining when overloading of the fracture plane occurs before the critical stage of the macro-crack. The found fracture energy then follows from the ultimate state of the fracture plane as applies for the AFPB-test and Eq. (9) applies. Also the 3ENF-test depends on a high enough loading of the parts for stress redistribution to make splitting possible. Thus the analysis in Sections 3 and 4 shows that K_{IIC} -values are fully dependent on choices of test equipment and dimensions of test specimens. These values should be compared, by a form-factor $f(a/W)$ to the case of a crack in an infinite medium which provides by definition the real K_{IIC} -value and thus is based on oblique crack extension of linear elastic fracture mechanics.

Thus the difference between the in [1] applied 3ENF- and AFPB-test is, that in the 3ENF-test the fracture plane is not overloaded and the shear stress remains the same at crack extension and thus also the value of K_{IIC} so that softening will follow the Griffith locus, while in the AFPB-test the loading of the fracture plane increases by crack extension, leading to overloading to the ultimate state and thus failure of the whole fracture plane (also outside the macro-crack tip region), acting as an apparent decrease of K_{IIC} as shown in Section 3. The AFPB-test further is unstable for initial long cracks, indicating that the test is not stiff enough to follow steeper softening lines for shorter crack lengths and thus is not able to measure the real maximal K_{IIC} -value at the top of the real critical loading curve for macro-crack extension and the test cannot be used for that purpose. Clearly at initial loading small crack extension is already to a long crack stable state. The mode I tests of [5] also lead to overloaded fracture planes, but these tests were stiff enough to show the whole loading and softening curve.

6. Comment and conclusion

- The compliance factor according to Eq. (1) should not be applied, because the solution whereupon it is based does not satisfy the Wu-fracture criterion and does not satisfy the equilibrium conditions of the isotropic wood-matrix.
- The too low value of $f(a/W)$ of [1] shows a too low estimate of G_{IIC} and indicates that not only the elastic energy change at collinear crack extension determines the fracture energy but also energy dissipation by small crack formation similar to plastic flow. This is confirmed by the ultimate state of the fracture plane, showing a constant ultimate stress on the intact part of the fracture plane.
- As known for wood, the fracture energy for pure mode I crack extension is equal to the elastic energy change by this crack extension. The derivation of the Wu-equation shows that the mixed mode loading, (and thus also mode II loading alone) is coupled to mode I. Both follow from tensile failure of the crack wall near the crack tip. For off axis crack extension by pure shear loading follows by this coupling: $G_{IIC} = 4G_{Ic}$. For any combined loading case, there always is tensile (mode I) failure in accordance with the Wu-equation, which is the real minimum energy solution of elastic fracture mechanics. Any other forced failure mode, is not according to the Wu-equation and thus needs more energy and is an upper bound solution, violating the failure criterion. The fracture energy then is not equal to the elastic energy change at crack extension.
- By not regarding oblique crack extension or plastic collinear crack extension at pure shear loading of the AFPB-test of [1], but treating this by elastic fracture mechanics by calculating the elastic energy change by the finite element virtual crack closure method, a two times too low ratio, thus: $G_{IIC} = 2G_{Ic}$ is possible. Analysis of test-data is necessary to refine this ratio value.
- The strength behaviour of a long crack with a high loaded fracture plane appears to be similar to softening behaviour after the first stage of passing the top of the curve. This occurs when the test equipment is not stiff enough to follow the softening curve.

- It is shown in [2], based on the softening data of [5], that for mode I, after the first stage of softening, due to small crack propagation and merging in the high loaded fracture plane, not K_I is constant, but the strength of the decreasing intact area of the fracture plane is determining. Thus not the nominal stress but the ultimate real stress f_t in the intact part of the fracture plane is determining for the ultimate load at that softening state.
- New is, that analysis of the AFPB-tests of [1] show that the same applies for mode II. Thus:- The in [1] measured apparent decrease of K_{IIc} for long cracks in the AFPB-tests, is for every crack length explained by the strength of the remaining intact part of fracture plane.
- The AFPB-test is unstable for long cracks, indicating that the test-equipment is not stiff enough to follow steep parts of the softening line for shorter crack lengths and thus is not able to show the real maximal K_{IIc} value of macro-crack extension at the top of the loading curve.

References

- [1] Yoshihara H. Mode II fracture mechanics properties of wood measured by the asymmetric four-point bending test using a single-edge-notched specimen. *Engng. Frac. Mech.* 2008;75:4727–39.
- [2] van der Put TACM. *A New Fracture Mechanics Theory of Wood*. New York: Nova Science Publishers, Inc.; 2011.
- [3] Sih GC, Paris PC, Irwin GR. On crack in rectilinearly anisotropic bodies. *Int. J. Fract. Mech.* 1965;1:189–203.
- [4] Susanti CME, Nakao T, Yoshihara H. Examination of the mode II fracture behaviour of wood with a short crack in an asymmetric four point bending test. *Eng. Fract. Mech.* 2011;78–16(November). 2775–2738.
- [5] L. Boström, Method of determination of the softening behaviour of wood, etc. Thesis, Report TVBM-1012, Lund, Sweden, 1992.
- [6] van der Put TACM. A continuum failure criterion applicable to wood. *J. Wood Sci.* 2009;55(5):315–22.